

Compact monolithically-integrated hybrid (de)multiplexer based on silicon-on-insulator nanowires for PDM-WDM systems

Sitao Chen, Yaocheng Shi, Sailing He, and Daoxin Dai*

Centre for Optical and Electromagnetic Research, State Key Laboratory for Modern Optical Instrumentation, Zhejiang Provincial Key Laboratory for Sensing Technologies, Zhejiang University, Zijingang Campus, Hangzhou 310058, China

**dxdai@zju.edu.cn*

Abstract: A compact silicon hybrid (de)multiplexer is designed and demonstrated by integrating a single bi-directional AWG with a polarization diversity circuit, which consists of an ultra-short polarization-beam splitter (PBS) based on a bent coupler and a polarization rotator (PR) based on a silicon-on-insulator nanowire with a cut corner. The present hybrid (de)multiplexer can operate for both TE- and TM- polarizations and thus is available for PDM-WDM systems. An 18-channel hybrid (de)multiplexer is realized with 9 wavelengths as an example. The wavelength-channel spacing is 400GHz (i.e., $\Delta\lambda_{\text{ch}} = 3.2\text{nm}$) and the footprint of the device is about $530\mu\text{m} \times 210\mu\text{m}$. The channel crosstalk is about -13dB and the total excess loss is about 7dB. The excess loss increases by about 1~2dB due to the cascaded polarization diversity circuit in comparison with a single bi-directional AWG.

©2015 Optical Society of America

OCIS codes: (130.0130) Integrated optics; (130.7408) Wavelength filtering devices; (130.3120) Integrated optics devices.

References and links

1. D. Dai and J. E. Bowers, "Silicon-based on-chip multiplexing technologies and devices for Peta-bit optical interconnects," *Nanophoton.* **3**(4–5), 283–311 (2014).
2. J. Wang, S. Chen, and D. Dai, "Silicon hybrid demultiplexer with 64 channels for wavelength/mode-division multiplexed on-chip optical interconnects," *Opt. Lett.* **39**(24), 6993–6996 (2014).
3. J. Wang, S. He, and D. Dai, "On-chip silicon 8-channel hybrid (de)multiplexer enabling simultaneous mode- and polarization-division- multiplexing," *Laser & Photon. Rev.* **8**(2), L18–L22 (2014).
4. M. K. Smit and C. Van Dam, "Phasar-based WDM-devices: principles, design and applications," *IEEE J. Sel. Top. Quantum Electron.* **2**(2), 236–250 (1996).
5. W. Bogaerts, D. Taillaert, P. Dumon, D. Van Thourhout, R. Baets, and E. Pluk, "A polarization-diversity wavelength duplexer circuit in silicon-on-insulator photonic wires," *Opt. Express* **15**(4), 1567–1578 (2007).
6. L. Chen, C. R. Doerr, and Y. Chen, "Polarization-diversified DWDM receiver on silicon free of polarization-dependent wavelength shift," *Optical Fiber Communication Conference. Optical Society of America*, 2012: OW3G. 7.
7. S. Pathak, M. Vanslebrouck, P. Dumon, D. Van Thourhout, and W. Bogaerts, "Compact SOI-based polarization diversity wavelength de-multiplexer circuit using two symmetric AWGs," *Opt. Express* **20**(26), B493–B500 (2012).
8. T. Barwicz, M. R. Watts, M. A. Popović, P. T. Bakich, L. Socci, F. X. Kärtner, E. P. Ippen, and H. I. Smith, "Polarization-transparent microphotonic devices in the strong confinement limit," *Nat. Photonics* **1**(1), 57–60 (2007).
9. H. Fukuda, K. Yamada, T. Tsuchizawa, T. Watanabe, H. Shinojima, and S. Itabashi, "Silicon photonic circuit with polarization diversity," *Opt. Express* **16**(7), 4872–4880 (2008).
10. J. Zhang, H. Zhang, S. Chen, M. Yu, G. Q. Lo, and D. L. Kwong, "A tunable polarization diversity silicon photonics filter," *Opt. Express* **19**(14), 13063–13072 (2011).
11. Y. Ding, L. Liu, C. Peucheret, J. Xu, H. Ou, K. Yvind, X. Zhang, and D. Huang, "Towards polarization diversity on the SOI platform with simple fabrication process," *Photon. Technol. Lett.* **23**(23), 1808–1810 (2011).
12. Y. Qin, Y. Yu, J. Zou, M. Ye, L. Xiang, and X. Zhang, "Silicon based polarization insensitive filter for WDM-PDM signal processing," *Opt. Express* **21**(22), 25727–25733 (2013).
13. L. Chen, C. R. Doerr, and Y. K. Chen, "Compact polarization rotator on silicon for polarization-diversified circuits," *Opt. Lett.* **36**(4), 469–471 (2011).

14. T. Tsuchizawa, K. Yamada, H. Fukuda, T. Watanabe, J. Takahashi, M. Takahashi, T. Shoji, E. Tamechika, S. Itabashi, and H. Morita, "Microphotonic devices based on silicon microfabrication technology," *IEEE J. Sel. Top. Quantum Electron.* **11**(1), 232–240 (2005).
15. W. Bogaerts, P. Dumon, D. V. Thourhout, D. Taillaert, P. Jaenen, J. Wouters, S. Beckx, V. Wiaux, and R. G. Baets, "Compact wavelength-selective functions in silicon-on-insulator photonic wires," *IEEE J. Sel. Top. Quantum Electron.* **12**(6), 1394–1401 (2006).
16. K. Sasaki, F. Ohno, A. Motegi, and T. Baba, "Arrayed waveguide grating of $70 \times 60 \mu\text{m}^2$ size based on Si photonic wire waveguides," *Electron. Lett.* **41**(14), 801–802 (2005).
17. D. Dai, L. Liu, L. Wosinski, and S. He, "Design and fabrication of ultra-small overlapped AWG demultiplexer based on alpha-Si nanowire waveguides," *Electron. Lett.* **42**(7), 400–402 (2006).
18. P. Dumon, W. Bogaerts, D. Van Thourhout, D. Taillaert, R. Baets, J. Wouters, S. Beckx, and P. Jaenen, "Compact wavelength router based on a Silicon-on-insulator arrayed waveguide grating pigtailed to a fiber array," *Opt. Express* **14**(2), 664–669 (2006).
19. S. Cheung, T. Su, K. Okamoto, and S. J. B. Yoo, "Ultra-Compact Silicon Photonic 512×512 25 GHz Arrayed Waveguide Grating Router," *IEEE J. Sel. Top. Quantum Electron.* **20**(4), 310–316 (2014).
20. J. Wang, Z. Sheng, L. Li, A. Pang, A. Wu, W. Li, X. Wang, S. Zou, M. Qi, and F. Gan, "Low-loss and low-crosstalk 8×8 silicon nanowire AWG routers fabricated with CMOS technology," *Opt. Express* **22**(8), 9395–9403 (2014).
21. D. Dai, L. Liu, S. Gao, D. Xu, and S. He, "Polarization management for silicon photonic integrated circuits," *Laser Photon. Rev.* **7**(3), 303–328 (2013).
22. H. Fukuda, K. Yamada, T. Tsuchizawa, T. Watanabe, H. Shinjima, and S. Itabashi, "Ultrasmall polarization splitter based on silicon wire waveguides," *Opt. Express* **14**(25), 12401–12408 (2006).
23. D. Dai and J. E. Bowers, "Novel ultra-short and ultra-broadband polarization beam splitter based on a bent directional coupler," *Opt. Express* **19**(19), 18614–18620 (2011).
24. J. Wang, D. Liang, Y. Tang, D. Dai, and J. E. Bowers, "Realization of an ultra-short silicon polarization beam splitter with an asymmetrical bent directional coupler," *Opt. Lett.* **38**(1), 4–6 (2013).
25. Z. Wang and D. Dai, "Ultrasmall Si-nanowire-based polarization rotator," *J. Opt. Soc. Am. B* **25**(5), 747–753 (2008).
26. M. Aamer, A. M. Gutierrez, A. Brimont, D. Vermeulen, G. Roelkens, J. Fedeli, A. Håkansson, and P. Sanchis, "CMOS compatible silicon-on-insulator polarization rotator based on symmetry breaking of the waveguide cross section," *IEEE Photon. Technol. Lett.* **24**(22), 2031–2034 (2012).
27. S. Chen, X. Fu, J. Wang, Y. Shi, S. He, and D. Dai, "Compact dense wavelength division (de)multiplexer utilizing a bidirectional Arrayed-waveguide Grating integrated with a Mach-Zehnder Interferometer," *J. Lightwave Technol.* **33**(11), 2279–2285 (2015).
28. D. Taillaert, P. Bienstman, and R. Baets, "Compact efficient broadband grating coupler for silicon-on-insulator waveguides," *Opt. Lett.* **29**(23), 2749–2751 (2004).

1. Introduction

A hybrid multiplexing technology has attracted intensive attention by combining multi-wavelengths, multi-modes, as well as dual-polarizations [1]. In this way, the link capacity can be enhanced to satisfy the increasing demand of the transmission capacity for optical fiber communication systems as well as on-chip optical interconnects. For the realization of any hybrid (de)multiplexing technology, hybrid (de)multiplexer is one of the most important key components. For example, in [2] a 64-channel hybrid (de)multiplexer combining wavelength division multiplexing (WDM) and mode-division-multiplexing (MDM) together is realized by using 16 wavelengths and four modes. A 8-channel hybrid (de)multiplexer has also been demonstrated with four modes and dual polarizations to enable polarization-division-multiplexing (PDM) and MDM simultaneously [3]. In this paper, we focus on the realization of a compact hybrid (de)multiplexer based on silicon-on-insulator nanowires for PDM-WDM systems.

In order to realize this kind of hybrid (de)multiplexer, one of the most straightforward method is using a polarization-beam splitter (PBS) cascaded by two wavelength-division-(de)multiplexers with N wavelength-channels, e.g., arrayed-waveguide gratings (AWGs), which is one of the most important components in various WDM modules and systems [4]. In this way, the input signals are first separated by a PBS to have two polarized beams (i.e., TE and TM), which then enter two AWGs separately. Finally there are $2N$ channels achieved with dual polarizations and N wavelengths. The problem is that the two AWGs are required to be designed respectively for TE- and TM- polarizations and it is difficult to make the two AWGs have identical wavelength alignments for all the channels due to fabrication errors.

An alternative way is using the so-called polarization-diversity technology by using the photonic integrated circuits (PICs) including PBSs as well as polarization rotators (PRs) [8].

In this way, one of the two polarization is rotated so that one can have two groups of signals with the same polarization states and consequently one only needs to design the AWG working for one polarization. Particularly, only one $N \times N$ AWG is needed by utilizing its bi-directional property. It is well known that the polarization-diversity technology has been developed as a general solution to overcome the severe polarization-dependence of PICs [5–12]. In [5], a very smart design is presented by using a two-dimensional grating coupler which plays the roles of a fiber-chip coupler, a PBS and a PR simultaneously. However, it might be not very convenient to be integrated with other functional devices on the same chip. In contrast, the method of utilizing on-chip PBSs and PRs is more compatible for photonic integration. In [6], a monolithically integrated dense WDM receiver chip on silicon was demonstrated by integrating a bi-directional AWG and a polarization-diversity circuit including a PBS and PR. In this design, the AWG is based on Si_3N_4 waveguides while the PBS is based on cascaded directional couplers of silicon waveguides [22] and the PR is based on adiabatic mode evolution with the assist of a tapered Si_3N_4 waveguide lying on top of the silicon waveguide [13]. The introduction of Si_3N_4 makes the fabrication slightly more complicated and also makes the device footprint larger than the pure-silicon design. For example, the footprint of the chip (with 10 wavelength-channels at 100GHz spacing) demonstrated in [6] is $8.0 \text{ mm} \times 2.5 \text{ mm}$. Therefore, it is desired to achieve a compact pure-silicon AWG with a polarization-diversity circuit.

In recent years, silicon photonics has been very popular in recent years because it allows photonic integrated devices to be fabricated cheaply using CMOS-compatible processes and naturally integrated with microelectronic chips. Furthermore, silicon-on-insulator (SOI) nanowires have ultra-high refractive index contrasts and ultra-sharp bending is enabled [14,15]. This helps achieve ultra-dense photonic integrated circuits (PICs), including AWGs [16–20]. It is also well known that SOI nanowires usually have very high birefringence resulting from the ultra-high refractive index contrast and the submicron cross section [21]. This definitely helps a lot to achieve ultra-compact on-chip polarization-handling devices (e.g., PBSs [22–24], PRs [25,26], and polarizers), which are the key elements for a hybrid (de)multiplexer used in a WDM-PDM hybrid multiplexing system.

In this paper, we present a silicon-based $(N + 1) \times (N + 1)$ bi-directional AWG (de)multiplexer integrated with a polarization-diversity circuit for realizing the WDM-PDM hybrid (de)multiplexing. With the present design, two orthogonal polarizations can be utilized and there are $2N$ channels available with N wavelengths only. This makes the link capacity doubled in comparison with a WDM system with N wavelength-channels. As an example, in this paper we design and fabricate a 10×10 bi-directional AWG (de)multiplexer integrated with a polarization-diversity circuit, which consists of a PBS based on a bent direction coupler [23,24], and a PR based on a SOI nanowire with a cut corner [25,26]. The present hybrid (de)multiplexer has 18 channels available with 9 wavelengths and the footprint of the whole structure is about $530\mu\text{m} \times 210\mu\text{m}$ only.

2. Structure and design

Figure 1(a)-1(b) shows the schematic configuration of the present hybrid (de)multiplexer, which consists of a bi-directional AWG and a polarization-diversity circuit including a PBS based on a bent direction coupler (see Fig. 2), and a PR based on a SOI nanowire with a cut corner (see Fig. 3). As shown in Fig. 1(a), the bi-directional AWG has $N + 1$ access optical waveguides at both sides. Among the $N + 1$ access optical waveguides at each side, one is used as an input waveguide and the others are used as output waveguides. Particularly, for the present case, the access waveguide at the inner-edge is chosen as the input waveguide in order to have a convenient layout design (avoiding any crossings). In this way, there are $2N$ output waveguides to receive $2N$ channels carried by N wavelengths ($\lambda_1, \lambda_2, \dots, \lambda_N$) and two polarizations (TE and TM), respectively. The polarization-diversity circuit used for the bi-directional AWG includes a PBS and a PR, as shown in Fig. 1(b). The input $2N$ channels of optical signals are separated into the TE-polarization group and the TM-polarization group by a broadband PBS. Each group has N wavelength channels ($\lambda_1, \lambda_2, \dots, \lambda_N$). The TM-

polarization group is then rotated and converted to TE polarization by using a broadband PR. These two groups of signals are then input to the two input waveguides of the bi-directional AWG and then demultiplexed respectively by the bi-directional AWG. Since the bi-directional AWG is symmetric, it is expected to have identical responses from the output waveguides for the inputs at both sides.

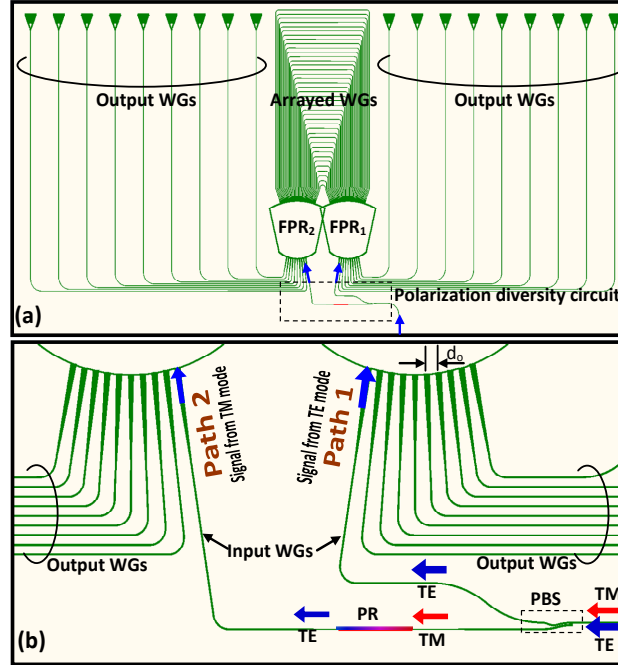


Fig. 1. (a) Schematic configuration of the present hybrid (de)multiplexer consisting of a bi-directional AWG and a polarization diversity circuit; (b) the enlarged view for the polarization diversity circuit connecting with the two input waveguides of the bi-directional AWG.

As example, in our case the channel spacing of the bi-directional AWG is chosen to be $\Delta\lambda_{ch} = 3.2\text{nm}$ ($\Delta f_{ch} = 400\text{GHz}$) and the channel number is $N = 9$. With this design, an 18-channel hybrid (de)multiplexer is enabled with 9 channels for TE polarization and 9 channels for TM polarizations. A 220nm-thick SOI wafer is used and the designed single-mode SOI nanowire has a cross section of $500\text{nm} \times 220\text{nm}$. The parameters of the designed bi-directional AWG are given as follows. The diffraction order is chosen as $m = 30$ to make the free spectral range (FSR) large enough to cover all the wavelength channels, i.e., $\text{FSR} > N\Delta\lambda_{ch}$. The path difference between the adjacent arrayed waveguides is $\Delta L = 19.64\mu\text{m}$, calculated with the formula $\Delta L = m\lambda_c/n_{eff}$, where λ_c is the central wavelength, and n_{eff} is the effective index of the fundamental mode in the arrayed waveguide. With this design, the FSR is about $29\mu\text{m}$, which is enough for 9 channels. The gap between the adjacent arrayed waveguides at the end connecting with the free propagation regions (FPRs) is chosen as 300nm to make the etching depth uniformly regarding the lag effect of the etching process. The end separation between the output waveguides is about $3.69\mu\text{m}$ and the length of the FPRs is $R_a = 100\mu\text{m}$. With this design, the footprint for the part including the arrayed waveguides and the two FPRs is about $440\mu\text{m} \times 190\mu\text{m}$.

The PBS used here is realized by using an asymmetric bent directional coupler proposed in [23], as shown in Fig. 2. The core widths for the bent waveguides in the coupling region are chosen optimally to make the phase matching condition satisfied for TM mode so that a complete cross-coupling happens when choosing the length for the coupling region appropriately. In contrast, there is no coupling almost for TE mode due to the huge birefringence of silicon nanowire waveguides. In the present example, the designed PBS has

the following parameters: the bending radii $R_1 = 20\mu\text{m}$ and $R_2 = 19.3\mu\text{m}$, the core widths $w_1 = 460\text{nm}$, $w_2 = 530\text{nm}$, the gap width $w_g = 205\text{nm}$, the length for the coupling region $L = 5.39\mu\text{m}$. Here the parameters for this PBS is slightly different from those reported in [23,24] because of the different upper-cladding or the top-silicon thickness.

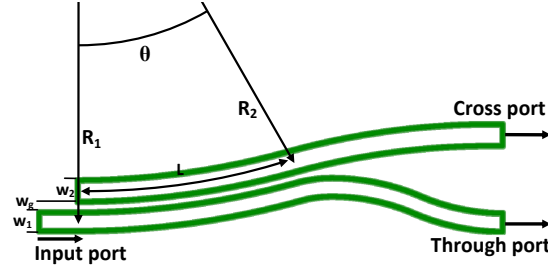


Fig. 2. Schematic configuration of the PBS based on a bent coupler.

The PR is achieved by breaking the symmetry of the cross section of the SOI nanowire waveguide [25], as shown in Fig. 3. According to the experimental results demonstrated in [26], we choose the following parameters: $H = 220\text{nm}$, $W = 200\text{nm}$, $W_e = 50\text{nm}$, $H_e = 70\text{nm}$, the length of the rotation region $L_c = 22\mu\text{m}$. For the input/output section, the waveguide widths are chosen as $w = 500\text{nm}$ and a $10\mu\text{m}$ -long linear taper is introduced to connect the sections with different widths. Here the shallow etched part has the same etch depth with the grating coupler so that no additional fabrication process is introduced.

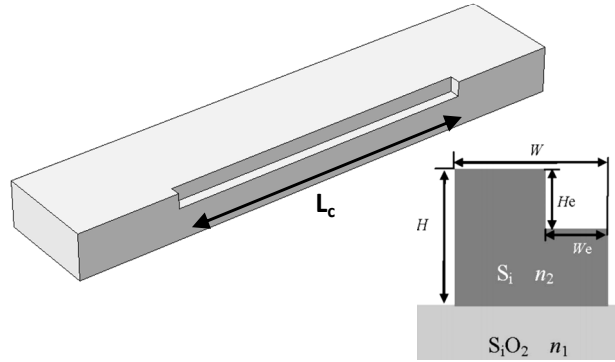


Fig. 3. Schematic configuration of the polarization rotator based on a SOI nanowire with a cut corner. Inset: the cross section of the waveguide at the rotation region.

3. Fabrication and measurement

For the fabrication of the present hybrid (de)multiplexer, the process was started from a 220nm -thick SOI wafer. E-beam lithography process with MA-N2403 photoresist was carried out to make the waveguide pattern, which was then transferred to the silicon layer with an inductively coupled plasma (ICP) etching process. Grating couplers were made with another shallow-etching process to achieve efficient coupling between the fibers and the chip. Finally PMMA photoresist with 300nm thickness was spin-coated on the top of the chip for protection.

For the characterization of the fabricated devices, in order to have reproducible fiber-chip alignment, in our measurement we did not use the popular setup with a tunable laser and a photodetector, which does not work well [27]. Instead, we used the setup including a broadband light source and an optical spectrum analyzer (OSA) so that the fiber alignment can be optimized by maximizing the total transmission power in a given wavelength band (e.g. ranging from 1535nm to 1565nm corresponding to the wavelength band of our AWG),

which was proved to be very reliable (as discussed in ref [27]). This has been proved to provide a reliable approach for normalizing the transmissions of the devices with respect to the transmission of the grating coupler [27]. The linear polarization state of the injected light is guaranteed by the polarization dependent grating coupler, which usually has a polarization extinction ratio of more than 20dB [28]. By using this measurement approach, the measured losses of the fabricated single-mode SOI nanowire with a cross section of $500\text{nm} \times 220\text{nm}$ are $\sim 2.2\text{dB/cm}$ for TE mode and $\sim 1.6\text{dB/cm}$ for TM mode. For the grating coupler, the excess losses (at the peak wavelength) are 4.5dB/coupler and 5.0dB/coupler for TE and TM polarizations while the 3dB bandwidths are estimated to be around 45nm and 60nm for TE and TM polarizations. The grating couplers on the same chip have excellent reproducibility according to our experiment results [27].

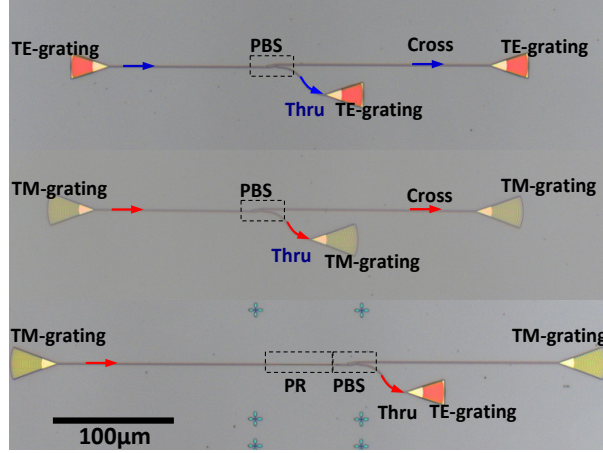


Fig. 4. Microscopic images of the fabricated structures to test the PBSs and PRs.

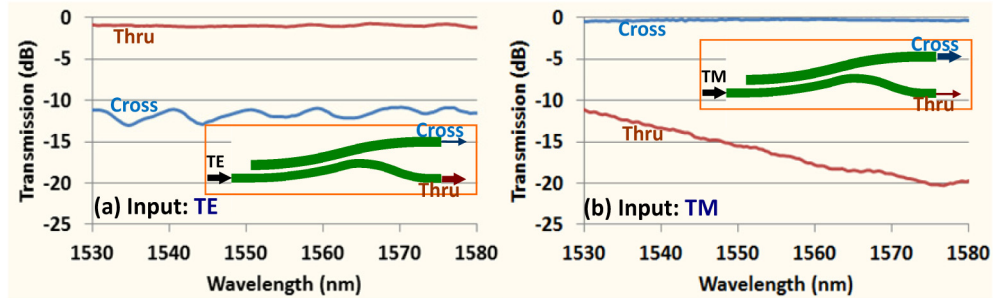


Fig. 5. Normalized measurement results for the PBS when the input is (a) TE, (b) TM polarization modes.

In order to characterize the PBS and the PR used for the hybrid (de)multiplexer, we include some test structures on the same chip, as shown in Fig. 4, regarding that the polarization-sensitivity of the grating coupler. We include a groups of PBSs with identical designs on the same chip while the grating couplers connected at the input/output ends are for TE or TM polarizations, so that the transmissions at the through- and cross- ports for TE- and TM- polarizations can be measured. Figure 5(a)-5(b) show the measurement results for the fabricated PBSs when the TE- and TM- polarized light is input respectively. These results are normalized with respect to the transmission of a straight waveguide with the corresponding grating couplers at both ends. It can be seen that the insertion loss is about 1dB for TE polarization and the extinction ratio is about 10dB over a wavelength band of 50nm ranging from 1530nm to 1580nm. For TM polarization, the excess loss is almost zero in the

wavelength range of 50nm and the extinction ratio is as high as 20dB at the wavelength of about 1575nm.

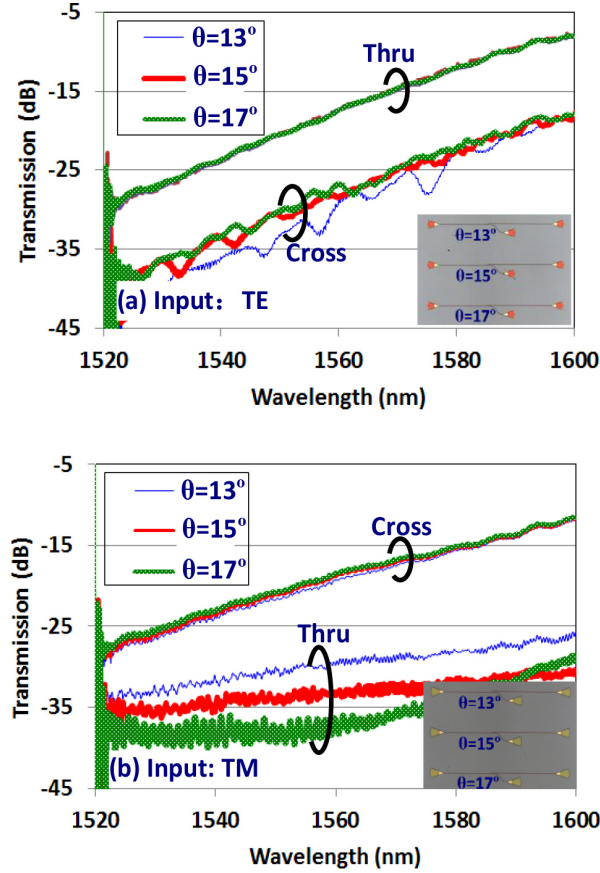


Fig. 6. (a) The fabricated PBSs with the grating couplers for TE polarization and the corresponding measured transmissions when the TE polarization mode is launched; (b) the fabricated PBSs with the grating couplers for TM polarization and the corresponding measured transmissions when the TM polarization mode is launched.

According to the theoretical prediction given in ref [23], the PBS based on a bent coupler has excellent fabrication tolerance for the variation of the waveguide dimension, which benefits to have reliable and reproducible devices. Here we also fabricated several PBSs with different angle-lengths ($\theta = 13^\circ, 15^\circ, 17^\circ$) for the bent coupling region to check the design optimization and the fabrication reproducibility (see the insets in Fig. 6(a)-(b)). Figure 6(a)-(b) show the original data of the measured transmissions for the fabricated PBSs with the grating couplers for TE polarization, and TM polarization, respectively. It can be seen that the transmissions at the cross port for TM polarization as well as the transmissions at the thru port for TE polarization are not sensitive to the angle-length θ , which is consistent with the theoretical prediction. The design with $\theta = 15^\circ$ is likely the optimal one according to the measurement results for the TM-polarization case. Meanwhile, one should also note that the transmissions does not change notably even when the angle length θ varies from 13° to 17° . It can be imaged that the transmissions should be very similar for the PBSs with the identical design on the same chip, which indicates that the PBS has good reproducibility. Note that these original data shown in Fig. 6(a)-(b) are not normalized with respect to the transmissions of the grating couplers, and the envelopes of these transmissions are defined by the grating coupler. Since there is no cross-coupling almost for the PBS in theory when the TE polarized light is launched, the transmission at the thru port for TE polarization is not sensitive to angle-

lengths θ and should be very similar to that for a straight waveguide with the same grating couplers. This is indeed observed from the measurement results shown in Fig. 6(a) even for the PBS with an angle length varying from 13° to 17° as predicted. The measurement results also indicate that also these grating couplers have identical transmissions almost.

For the characterization of PRs, the designed photonic integrated circuit consists of a PR connected with a PBS based on a bent coupler, as shown in Fig. 4. At the input end, a TM grating coupler is connected. At the output ends, a TE-type grating coupler and a TM-type grating coupler are connected at the through port and the cross port of the PBS, respectively. In this way, one can characterize how the PR modifies the polarization state of the light. Figure 7 shows the measurement result for the PR, which is normalized by the transmission of a PBS with grating couplers. It can be seen that the mode conversion efficiency from TM-polarization to TE-polarization is quite good in the wavelength range from 1530nm to 1550nm, with an insertion loss less than 1dB from TM mode to TE mode. The residual TM polarization mode (as indicated by the TM \rightarrow TM transmission shown in Fig. 7) is about -8dB with the reference of the input TM mode. This means about 15% of the input TM mode is unconverted and nearly 85% conversion efficiency from TM polarization to TE polarization is achieved. The polarization conversion efficiency decreases notably and the insertion loss increases to ~ 2 dB at the longer wavelength (e.g., $\lambda > 1560$ nm). Such performance is comparable with the results in ref [26], except that the central wavelength has some blue shift. This is due to the difference of the upper-cladding material and thickness as well as the waveguide-width deviation. According to the theoretical analysis in ref [26], the fabrication tolerance to achieve an 85% conversion efficiency is about ± 10 nm for the width variation. In the present case, the relatively poor performance mainly depends on the challenge of controlling the ultra-small feature size (about 50nm) accurately, which is relying on an alignment step. Therefore, one should control the fabrication process very carefully. In our configurations, all of the unwanted residual polarization mode will be filtered out by the polarization-selective grating couplers connected at the ends of the AWG. Thus, the residual TM-polarization light will not introduce significant crosstalk (which will be seen from the measured spectral responses of the AWG shown below).

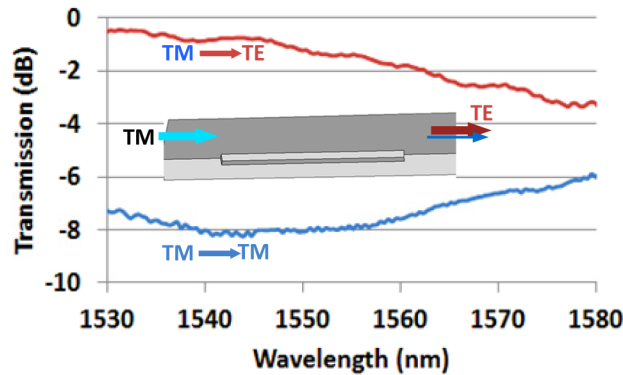


Fig. 7. Normalized measurement results for the transmissions (TM \rightarrow TE, and TM \rightarrow TM) for the PR when TM polarization mode is input.

Figure 8 shows the optical micrographs for the fabricated hybrid (de)multiplexer for PDM-WDM systems, including a polarization diversity circuit and a bi-directional AWG. The footprint of the present (de)multiplexer is about $530\mu\text{m} \times 210\mu\text{m}$ (not including the expanded parts of the output waveguides), which is only slightly larger than a single AWG. In order to launch the TE-polarized and TM-polarized light through grating couplers, we add an additional polarization beam combiner (PBC) in front of the hybrid (de)multiplexer, as indicated in Fig. 8. Two grating couplers for TE and TM polarizations are connected at the two input ends of the PBC respectively.

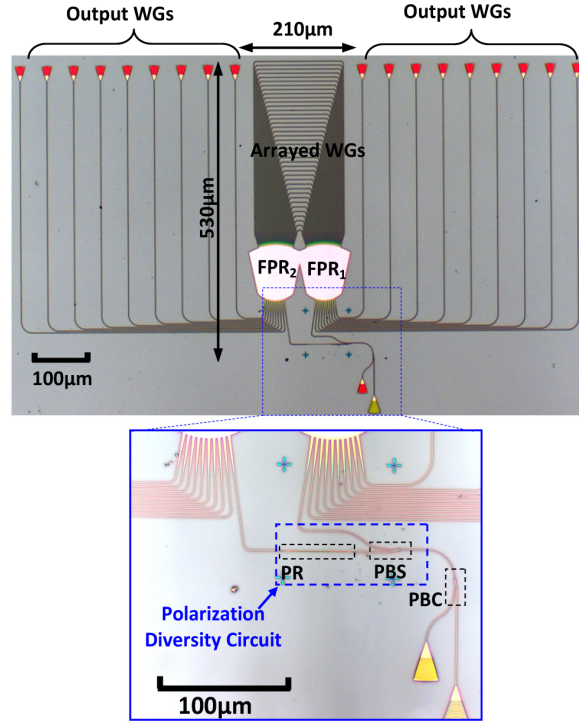


Fig. 8. Microscopic image of the fabricated hybrid (de)multiplexer consisting of a bi-directional AWG and a polarization diversity circuit.

Figure 9 shows the measured spectral responses for the whole structure, including a PBC, PBS, PR, and bi-directional AWG (as shown in Fig. 8). The spectrum is normalized by the transmission of a straight waveguide with grating couplers on the same chip. The solid curves are for the channels output from the ports at the left side, whose signals originate from the input TE mode, while the dashed curves are for the channels output from the ports at the right side, whose signals originate from the input TM mode. It can be seen that these two groups of channels are aligned very well with nearly zero polarization dependent wavelength (PDL). This is guaranteed intrinsically by such a bi-directional AWG working as two AWGs sharing the identical dispersion arrayed waveguide grating. The 3dB bandwidth is about 1.16nm and the channel crosstalk is about -13dB for the central channel (which is due to the fabrication induced phase errors). It can also be seen the fabricated device has quite low polarization dependent loss (PDL). From the measurement result for the PBS and PR shown in Fig. 5 and Fig. 7, one sees that the loss for TE polarization is mainly from the PBS while the loss for TM polarization is mainly from the PR. It is estimated that the PDL for the short wavelength ($\sim 1530\text{nm}$) is about 0.1dB and the PDL for the long wavelength ($\sim 1560\text{nm}$) is about 0.4dB, which is very consistent with the PDL shown in the measured responses given in Fig. 9. For the central channel #6, which is located at the central position of the input/output port, the excess loss is about 7dB for both polarizations. Apparently the excess loss is mainly from the bi-directional AWG and the polarization diversity circuit. Here the excess loss for the bi-directional AWG is estimated to be about 5~6dB. For the group of TE-mode signals, both PBC and PBS contribute about 1~2dB excess loss, as shown in Fig. 5(a). In contrast, for the group of TM mode signals, the excess loss is mainly from the PR (shown in Fig. 7). It can be seen that the excess loss is <1dB in the short wavelength range from 1530nm to 1550nm while the excess loss is 1~2dB in long wavelength range from 1550nm to 1560nm. Additionally, the PBC/PBS contribute an excess loss of <1dB (shown in Fig. 5(b)).

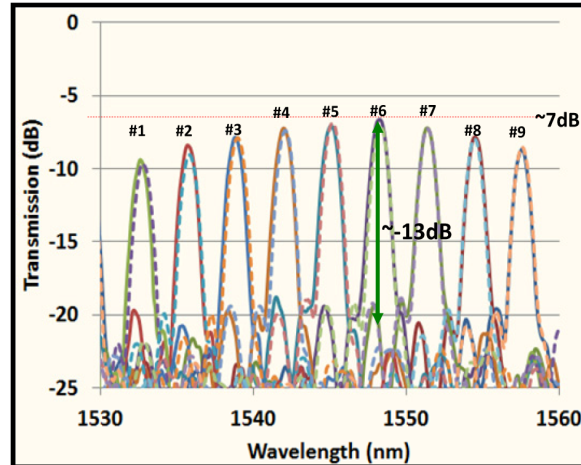


Fig. 9. Measured results of the fabricated hybrid (de)multiplexer with a channel spacing of 400GHz, which are normalized by the transmission of a straight waveguide with grating couplers on the same chip. Dashed lines are for the channels originating from the TM polarization, while the solid lines are for the channels originating from the TE polarization.

4. Conclusion

In summary, we have designed and demonstrated a compact silicon hybrid (de)multiplexer for PDM-WDM systems by integrating a single bi-directional AWG with a polarization diversity circuit. The polarization diversity circuit consists of a $\sim 10\mu\text{m}$ -long PBS based on a bent coupler and a $\sim 22\mu\text{m}$ -long PR based on a SOI nanowire with a cut corner. The PBS has an extinction ratio of $>10\text{dB}$ over a broad band ranging from 1530nm to 1580nm, which is similar to the results shown previously. For TM polarization, the excess loss is almost zero in the wavelength range of 50nm and the extinction ratio is as high as 20dB at the wavelength of about 1575nm. For the PR, the conversion efficiency from TM polarization to TE polarization is about 85% at the central wavelength and the performance can be improved further with better fabrications. With such a polarization diversity circuit as well a bi-directional AWG, we have achieved a hybrid (de)multiplexer operating for dual polarizations to make the channel number doubled. The present design with a bi-directional AWG guarantees a quite low PD λ because both polarizations share the identical dispersive waveguide grating. As an example, an 18-channel hybrid (de)multiplexer with 9 wavelengths has been realized with a channel spacing of 400GHz (i.e., $\Delta\lambda_{\text{ch}} = 3.2\text{nm}$). Definitely the channel spacing can be reduced to be dense (e.g., 1.6nm or 0.8nm) to have more wavelength channels in a given wavelength band. The present device has a footprint of $530\mu\text{m} \times 210\mu\text{m}$ (including the bi-directional AWG and the polarization diversity circuit). For the fabricated device, the channel crosstalk is about -13dB and the excess loss is about 7dB for both polarizations at the central channel ($\sim 1545\text{nm}$). The cascaded polarization diversity circuit introduces an excess loss of 1~2dB. As the polarization diversity circuit works in a broad band, it is possible to cover more wavelength channels and thus large number of channel is available potentially.

Acknowledgment

This project was partially supported by a 863 project (No. 2011AA010301), the Nature Science Foundation of China (No. 61422510, 91233208, and 6141101056), the Program of Zhejiang Leading Team of Science and Technology Innovation (2010R50007), the Doctoral Fund of Ministry of Education of China (No. 20120101110094), and the Fundamental Research Funds for the Central Universities.